Experimental Cell Research 410 (2022) 112946

Contents lists available at ScienceDirect

Experimental Cell Research

journal homepage: www.elsevier.com/locate/yexcr

Research article

Hemin enhances radiosensitivity of lung cancer cells through ferroptosis

Waleed Abdelbagi Almahi [a,b,c], K.N. Yu [d,e], Fathelrahman Mohammed [f], Peizhong Kong [a], Wei Han [a,g,*]

[a] Anhui Province Key Laboratory of Medical Physics and Technology, Institute of Health and Medical Technology, Hefei Institutes of Physical Science, Chinese Academy of Sciences, Hefei, 230031, People's Republic of China
[b] Science Island Branch of Graduate School, University of Science and Technology of China, Hefei, 230026, China
[c] Sudan Atomic Energy Commission, Nuclear Applications in Biological Sciences Institute, Radiobiology and Cancer Researches Department, Khartoum 11111, P.O Box 3001, Sudan
[d] Department of Physics, City University of Hong Kong, Tat Chee Avenue, Kowloon Tong, 999077, Hong Kong, People's Republic of China
[e] State Key Laboratory in Marine Pollution, City University of Hong Kong, Tat Chee Avenue, Kowloon Tong, 999077, Hong Kong, People's Republic of China
[f] CAS Key Laboratory of Soft Matter Chemistry, Department of Polymer Science and Engineering, University of Science and Technology of China, Hefei, 230026, Anhui, China
[g] Hefei Cancer Hospital, Chinese Academy of Sciences, Hefei, 230031, People's Republic of China

ARTICLE INFO

Keywords:
Ferroptosis
Hemin
Radiosensitivity
ROS
GPx4
FTH1
Bilirubin

ABSTRACT

The principle underlying radiotherapy is to kill cancer cells while minimizing the harmful effects on non-cancer cells, which has still remained as a major challenge. In relation, ferroptosis has recently been proposed as a novel mechanism of radiation-induced cell death. In this study, we investigated and demonstrated the role of Hemin as an iron overloading agent in the generation of reactive oxygen species (ROS) induced by ionizing radiation in lung cancer and non-cancer cells. It was found that the presence of Hemin in irradiated lung cancer cells enhanced the productivity of initial ROS, resulting in lipid peroxidation and subsequent ferroptosis. We observed that application of Hemin as a co-treatment increased the activity of GPx4 degradation in both cancer and normal lung cells. Furthermore, Hemin protected normal lung cells against radiation-induced cell death, in that it suppressed ROS after radiation, and boosted the production of bilirubin which was a lipophilic ROS antioxidant. In addition, we demonstrated significant FTH1 expression in normal lung cells when compared to lung cancer cells, which prevented iron from playing a role in increasing IR-induced cell death. Our findings demonstrated that Hemin had a dual function in enhancing the radiosensitivity of ferroptosis in lung cancer cells while promoting cell survival in normal lung cells.

1. Introduction

Lung cancer is the leading cause of cancer death in the world [1]. Fractionated doses have been widely used in radiotherapy to treat lung cancer patients. However, it is well established that DNA repairing pathways can occur in cells between dose fractions. Previous studies have reported possible mechanisms linked to radioresistance such as high DNA repair capacity, high cellular antioxidant capabilities, alterations of cell cycle profiles, epithelial-mesenchymal transition, and activation of a pathway associated with resistance to apoptosis [2]. Remarkably, radioresistance has remained a fundamental challenge in radiotherapy, which has affected the efficiency of lung cancer treatments [3–5].

While radiation-induced apoptosis and senescence of tumor cells have been well studied, other forms of cell death are less examined. Ferroptosis has recently been recognized as a new form of radiation-induced cell death [6–11]. Ferroptosis is a non-apoptotic form of cell death that relies on intracellular iron and occurs when imbalanced reactive oxygen species (ROS) assault the cell membrane and cause phospholipid polyunsaturated fatty acids (PUFA) peroxidation [12]. Subsequently, the glutathione peroxidase 4 (GPx4) enzyme utilizes glutathione and acts as a key regulator of lipid peroxidation [13–15]. However, cancer cells can express sufficient endogenous antioxidants, such as glutathione, heme oxygenase-1 (HO-1) and GPx4, to protect

* Corresponding author. Anhui Province Key Laboratory of Medical Physics and Technology, Institute of Health and Medical Technology, Hefei Institutes of Physical Science, Chinese Academy of Sciences, Hefei, 230031, People's Republic of China.
E-mail addresses: Waleed.a.a.almahi@gmail.com (W.A. Almahi), peter.yu@cityu.edu.hk (K.N. Yu), fathy.19867@gmail.com (F. Mohammed), gckongpz@163.com (P. Kong), hanw@hfcas.ac.cn (W. Han).

https://doi.org/10.1016/j.yexcr.2021.112946
Received 20 March 2021; Received in revised form 16 November 2021; Accepted 21 November 2021
Available online 24 November 2021

them from oxidative stress, which is associated with tumor progression and development [13,16]. Several studies have shown that GPx4 plays a significant role in chemotherapy and radiotherapy [14,15]. Therefore, designing new strategies to overcome this resistance in radiotherapy targeting the depletion of glutathione peroxidase 4 (GPx4) would be of clinical value.

Previously, Hemin was used as an intracellular iron source to promote ferroptosis in platelets via ROS-regulated proteasome activity [17]. Hemin has been shown to upregulate heme oxygenase-1 (HO-1) by degrading the nuclear transcription factors BTB and CNC homology 1 (BACH1). A heme-binding transcription factor, BACH1, is required for the appropriate regulation of the oxidative stress response and metabolic pathways related to heme and iron [18,19]. BACH1 has also been shown to regulate HO-1, FTH1, and other genes involved in oxidative stress [19–21]. HO-1 is considered a rate-limiting enzyme in heme breakdown that produces free iron, carbon monoxide and biliverdin/bilirubin [22]. The high level of HO-1 in cells has been postulated to protect cells from oxidative stress [23]. Hemin breakdown produces iron (Fe^{2+}) as an oxidant and biliverdin (BV)/bilirubin (BR) as an antioxidant [24,25]. Free iron can mediate an oxidative response involving free radicals or hydrogen peroxide via Fenton's reaction and the Haber-Weiss reaction [17,25,26]. When ionizing radiation interacts with water in cells, free radicals and hydrogen peroxide are generated, which can then interact with free iron to "amplify" the effects of ROS.

The heavy subunit of ferritin is encoded by the gene FTH1 as the main intracellular iron storage protein. This protein is made of 24 heavy and light ferritin chain subunits. Each FTH1 has the capacity to hold up to 4500 ferrous iron atoms [27]. Ferritin stores iron in a soluble and harmless form by converting Fe^{2+} to Fe^{3+}. Therefore, FTH1 avoids oxidative damage induced by Fenton reactions generating ROS, which can cause damages to proteins, lipids and other cellular components. Overexpression of FTH has been used to investigate the reduced quantity of redox-active iron [26,28–35]. Biliverdin is another byproduct of Hemin degradation that is transformed to Bilirubin (BR) by the Biliverdin reductase enzyme (BVR). Bilirubin has been identified as a lipophilic scavenger of ROS that may protect polyunsaturated fatty acid membranes from lipid peroxidation. Bilirubin may re-produce biliverdin when it reacts with these ROS [36–38].

In this study, we explored the impact of Hemin's dual functions on fractionated irradiation of lung normal and cancer cells with a view to enhance the efficacy of radiotherapy. We examined the outcomes of combinations of treatment with Hemin and ionizing radiation, including increased ferroptosis radiosensitivity of lung cancer cells via enhancing ROS production, lipid peroxidation and induction of GPx4 degradation. Hemin, on the other hand, protects normal lung cells from ionizing radiation via elevating bilirubin levels and shields iron by increasing FTH1 expression, which is suggested to be related to the reduced overall ROS in normal cells. Our findings have great potential contributions to enhancements in the efficacy of radiotherapy.

2. Materials and methods

2.1. Cell culture and reagents

The human NSCLC cell lines A549, H460, H1299, Calu-1, and normal human cell lines Beas-2B, MRC5 and HFL1 were purchased from the Cell Bank of Type Culture Collection of the Chinese Academy of Sciences (Shanghai, China). The A549, H1299, HFL1 and Calu-1 cell lines were cultured in RPMI 1640 medium, and H460, MRC5 and Beas-2B were cultured in DMEM medium (HyClone; GE Healthcare Life Sciences, Logan, UT, USA). All culture media were supplemented with 10% fetal bovine serum (FBS, HyClone), 100 μg/mL streptomycin and 100 U/mL penicillin (Gibco, Carlsbad, CA, USA). The cells were maintained at 37 °C in a humidified incubator with 5% CO_2 and 95% air. All cell lines were free of mycoplasma. Hemin (20 mM) and Bilirubin (BR, Sigma, USA), protein synthesis inhibitor Cycloheximide (CHX, Sigma), Ferrostatin-1 (5 mM, Sigma), liproxstatin-1 (10 μM, Sigma), necrostatin-1 (5 μM, from MCE), RSL3 and ZVAD-fmk (from MCE), proteasome inhibitor MG132 (Sigma, St Louis, MO, USA) and C11 BODIPY 581/591 (Invitrogen) were dissolved in DMSO. The transfection reagent RNAfit was from HANBIO (HB-RF-1000, China). The Bilirubin assay kit was from BioAssay System (USA).

2.2. Irradiation

The X-ray Irradiator (XSZ-220/20, Kangjia, Dandong, China) with a dose rate of 1.89 Gy/min was used to irradiate cells and xenograft athymic nude mice with a series of doses (0–10 Gy) or fractionated doses of 2 Gy/day.

2.3. Colony formation assay

The cells were plated into a 24-well plate at a density of 200–300 cells/well, then treated with Hemin and irradiation. The cells were co-cultured with Hemin (0–80 μM) and/or Ferrostatin-1(5 μM), liproxstatin-1(10 μM), ZVAD-fmk (5 μM) and necrostatin-1 (5 μM) for 2 h prior to irradiation. Ten to twelve days after IR, the cells were washed with PBS and fixed for staining with 1% crystal violet for 2 h, and the colonies containing ≥50 cells were then counted. Relative Plating Efficiency (PE) was calculated for each group. The survival fraction was calculated by normalization to appropriate relative control groups with the relative Plating Efficiency (PE). Survival curves were created with GraphPad Prism 8.0.1 software (GraphPad Prism Software, Inc., San Diego, CA, USA).

2.4. Cell viability assay

About 3–5 × 10^3 of cells were seeded overnight and followed with Hemin treatment before exposed to 3 × 2 Gy/day. In some experiments, the cells were transfected in 96-well plate with siRNAs for 12 h, then treated with Hemin (80 μM) for 2 h before radiation for 3 × 2 Gy/day. Two to three days after irradiation, cell viability was assessed with a Cell Counting Kit-8 (ApexBio, Houston, TX, USA). According to the manufacturer's protocol, 200 μL of CCK-8 working solution were added to each well and incubated for 40 min at 37 °C. Absorbance at 450 nm wavelength was measured with a Microplate Reader (Varioskan Flash, Thermo Fisher, Waltham, MA, USA). The relative cell viability was determined with GraphPad Prism 8.0.1 software.

2.5. Western blot

The total protein was homogenized with cold RIPA lysis buffer (Beyotime Biotechnology, Shanghai, China), and the concentration of protein was determined with a bicinchoninic acid (BCA) protein assay kit (Beyotime Institute of Biotechnology). The proteins from cell lysates (40–60 μg) were then separated with 8–12% sodium dodecyl sulfate-polyacrylamide gel electrophoresis (SDS-PAGE). Proteins were transferred to PDVF membranes (Merck Millipore, Darmstadt, Germany). The membranes were blocked with 5% skim milk (BD/Difco, Sparks, MD, USA) for 1 h, and then incubated with different primary antibodies at 4 °C overnight. The primary antibodies used were: anti-GPx4 (1:1000, ZEN-BIO, China), anti-ubiquitin (Proteintech, China, 1:600), BACH1, HO-1 and Tubulin (1:1000, Protein Tech Group), FTH1 (Abclonal). After washing with TBST, blots were incubated with IRDye-conjugated secondary antibodies (1:10000, Li-COR Biosciences, Lincoln, NE, USA) for 1 h at room temperature. Images of immunoreactive bands were captured with Odyssey CLx Infrared Imaging system (Li-COR Biosciences).

2.6. Immunoprecipitation (IP)

Immunoprecipitation was performed to identify GPx4 ubiquitination

as previously described [39]. Briefly, cells were lysed completely in 150 μl buffer (2% SDS, 150 mM NaCl, 10 mM Tris-HCl, pH 8.0) with 2 mM sodium orthovanadate, 50 mM sodium fluoride, 100 mM iodoacetamide (IAA, deubiquitylation inhibitor) and protease inhibitors. Cells were boiled for 10 min and sonicated before incubation at 4 °C for 30–60 min in rotation with 1350 μl dilution buffer (10 mM Tris-HCl, pH 8.0, 150 mM NaCl, 2 mM EDTA, 1% Triton-100). Anti-Glutathione Peroxidase 4/GPX4 Antibody (E−12), agarose bead-conjugated antibody AC from Santa Cruz (sc-166570 AC), was added to 4 mg of prepared cell lysates for immunoprecipitation for 2–3 h at 4 °C. The resin samples were washed three times with 1 ml washing solution (10 mM Tris-HCl, pH 8.0, 1 M NaCl, 1 mM EDTA, 1% NP-40) before being boiled with 2X SDS loading buffer. For immunoblotting analysis, samples were separated with 8–10% SDS-PAGE. For ubiquitination detection, 8% SDS-PAGE was used for H460 cells and 10% for A549 cells. Ubiquitin was plotted with 1:600 antibodies.

2.7. RT-PCR

One Step SYBR® PrimeScriptTM RT-PCR Kits (Takara Bio, Dalian, China) was used for RT-qPCR with Roche 480 Light Cycler (Roche, Basel, Switzerland). The following primers were used for PCR amplification: 5′-GAGGCAAGACCGAAGTAAACTAC-3′, 5′-CCGAACTGGTTACACGGGAA-3’ (GPx4) from (genewiz, China); and, 5′-GGAGCGAGATCCCTCCAAAAT-3′, 5′-GGCTGTTGTCATACTTCTCATGG-3’ (GAPDH) and 5′- AAGACTG CGTTCCTGCTCAAC-3′, 5′- AAAGCCCTACAGCAACTGTCG-3’ (HO-1) from (GENERAL BIOSYSTEM). GAPDH was used to normalize the total mRNA, and data analysis was performed with the $2^{-\Delta\Delta Ct}$ method to calculate the changes between groups.

2.8. Small Interfering RNA transfection

Cells were transfected with small interfering RNA or negative control RNA sequence (siCont) and transfection reagent RNAfit from HANBIO. The target sequences were as follows. siGPx4#1: 5′-UUCGAUAUGUU-CAGCAAGATT-3’; 5′-UCUUGCUGAACAUAUCGAATT-3’. siGPx4#2: 5′-GGC AAG ACC GAA GUA AAC UUU -3’; 5′- UUCCGUUCUGGCUU-CAUUUGA -3’. siFTH1#1: 5′-GAAUCAGUCACUACUGGAACdTdT-3′; 5′-GUUCCAGUAGUGACUGAUUCdTdT-3′. siFTH1#2: 5′-GUCCAUGU-CUUACUACUUUTT-3′; 5′-AAAGUAGUAAGACAUGGACTT-3′. The sequences of siCont were: 5′-UUCUCCGAACGUGUCACGUTT-3’; 5′-ACGUGACACGUUCGGAGAATT-3’.

2.9. Immunofluorescence

Cells were washed with PBS and fixed with 4% paraformaldehyde, then permeabilized and blocked with TNBS solution (PBS supplemented with 0.1% Triton X-100 and 1% FBS) for 1 h. The cells were incubated with specific anti-GPx4 (1:200) at 4 °C overnight. After rinsing with TNBS, the cells were incubated with Goat Anti-Rabbit IgG H&L (TRITC) (1:1000, Abcam) at 37 °C for 1 h. DAPI (5 mg/mL, Sigma-Aldrich) was used to stain the nuclei. Images of cells were captured with a fluorescence microscope (Leica DMI 4000B).

2.10. C11 581/591 BODIPY imaging

Cells (5×10^3) were seeded into each well of 24-well plates with a glass coverslip one day before the experiment. Next, the cells were treated with Hemin and/or ferrostatin-1 (5 μM) followed by 3 × 2 Gy/day irradiation. At 24 h after the last fraction, the medium was removed and the cells were washed with HBSS and incubated with C11 BODIPY 581/591 (5 μM in HBSS) at 37 °C for 10 min. After removing C11 BODIPY 581/591, fresh HBSS was added. Each cover slip was taken out and mounted in HBSS on a microscope slide for microscopic imaging.

2.11. Flow cytometer

Cells were treated with C11 BODIPY 581/591 (5 μM) for lipid peroxidation detection at 24 h after (3 × 2 Gy) irradiation. For ROS detection, cells were treated with 2′,7′-Dichlorofluorescin Diacetate DCFH-DA (10 μM) 10 min before IR (2 Gy). After 20 min incubation, the dye was removed and the cells were trypsinized and suspended in PBS for flow cytometry. The measurement of 20,000 cells was performed with a flow cytometer on the FL1 detector.

2.12. Bilirubin (BR) measurement

Cells were cultured in a medium with 2% FBS and treated with Hemin (80 μM), then washed with PBS after irradiation immediately. Cells in suspension were lysed in 150 μl of PBS with proteasome inhibitors and sonicated. The lysates were then centrifuged and the total protein in the supernatant was measured with BCA. Bilirubin in 500 μg of total protein lysate was measured according to company protocol (Bioassay).

2.13. Xenograft model

Experiments using the xenograft mouse model adhered to all relevant ethical regulations regarding animal research. Male 4–5 weeks old athymic nude mice were purchased from Model Animal Research Center of Nanjing University (Nanjing, China). The experiments involving all the animals were approved by the Ethical Committee of Experimental Animals of Hefei Institutes of Physical Science, Chinese Academy of Sciences. About 5×10^6 A549 cells suspended in 100 μl PBS were injected into mice subcutaneously. When the tumor reached 50–100 mm^3, the mice were separated randomly into different treatment groups. Tumors were irradiated with six fraction doses of 2 Gy/12 h. Hemin was dissolved in dimethyl sulfoxide (DMSO) and diluted in PBS, then injected into tumors at a dose of 20 mg/kg (50 μL) twice at 2 h before exposed to three fractions of irradiation. The tumor volume was measured 2 times per week until the end of the experiment and calculated according to the equation: volume = length × $width^2$ × 1/2.

2.14. Statistical analysis

All of the experiments were performed three times. The data were presented as mean ± SD. Differences between groups were assessed with 2-way ANOVA or one-way ANOVA with GraphPad Prism 8 depending on the experimental design, and statistically significance was considered at $p < 0.05$ (*) and ≤0.01 (**).

3. Results

3.1. Hemin enhanced radiosensitivity of lung cancer cells

A colony formation assay was performed in order to determine whether Hemin could enhance radiosensitivity in lung cancer cells. As shown in Fig. 1a, there is a clear decrease in the survival fraction of irradiated A549 and H460 cell lines treated with Hemin when compared to the control. Since cancer cells are more sensitive to low-doses (2 Gy) than normal cells, a fractionated strategy was used in radiotherapy for total radiation dosage. Therefore, we decided to investigate whether Hemin increased the sensitivity after fractionated irradiation. We found that Hemin significantly induced more cell death in response to fractioned radiation (2 Gy/day) as shown in Fig. 1b. This result demonstrated that Hemin enhanced radiosensitivity in Hemin-dependent manner.

Interestingly, as shown in Fig. 1c and d, Hemin has a protective role in non-cancer cells, such as normal lung cells (Beas-2B, MRC5 and HFL1). Clonogenic survival results showed that 40 and 80 μM Hemin could significantly protect Beas-2B cells from radiation-induced cell

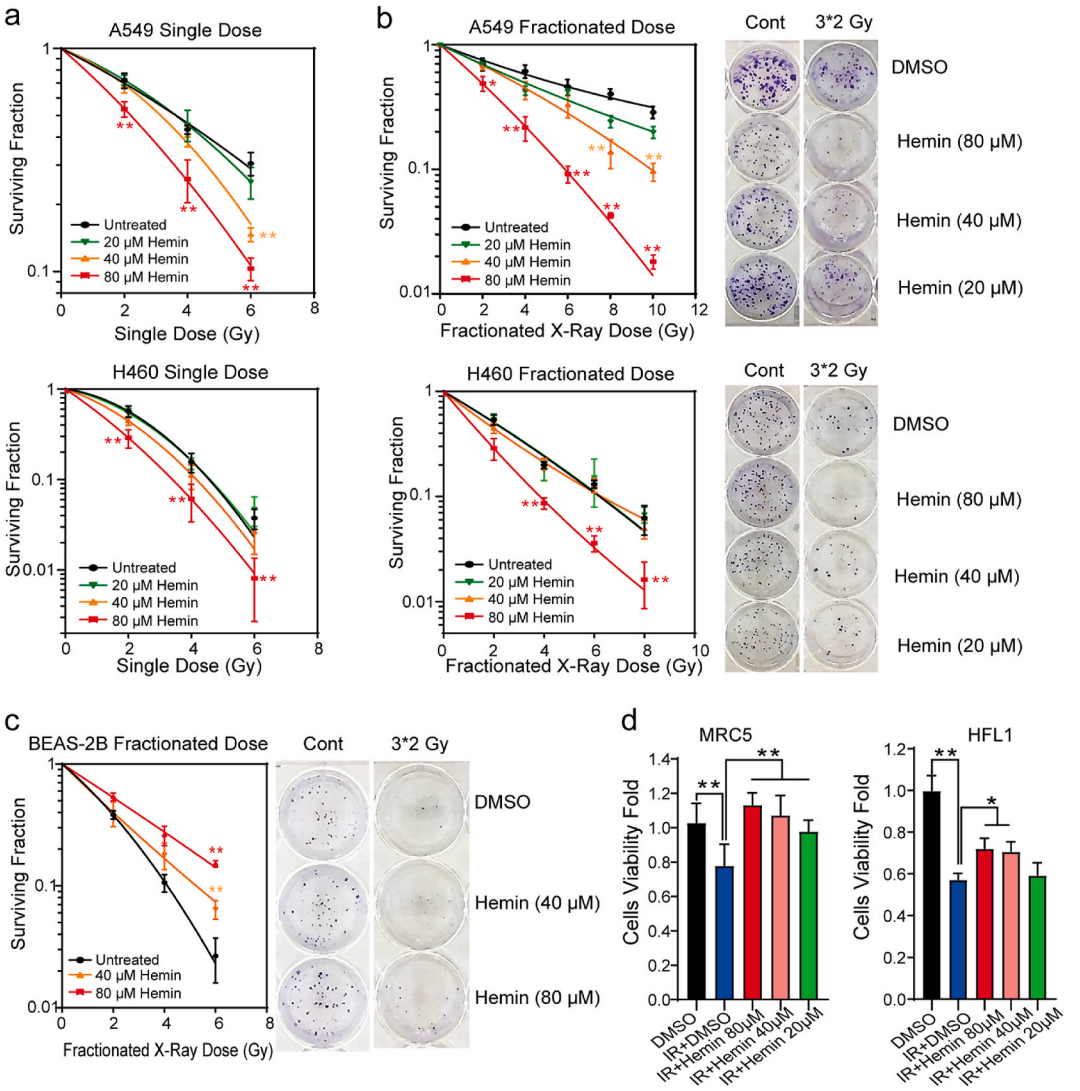

Fig. 1. Hemin enhanced radiosensitivity of lung cancer cells. (**a**) Colony survival curves of A549 and H460 cell lines treated with Hemin after exposure to IR with a single dose (2–8 Gy) or (**b**) fractionated radiation dose (2 Gy/day). (**c**) Colony survival curves of Beas-2B cells treated with 40 or 80 μM Hemin at 2 h before irradiation (2 Gy/day). The curves were normalized with PE for relative unirradiated control. (**d**) Cell viability was determined with CCK-8 two days after the last IR dose of 3 × 2 Gy/day. Error bars indicate ±SD and means from three independent repeats. *P-value,* * ≤ *0.05 &* ** ≤ *0.01.*

death (Figure 1c). Furthermore, cell viability test (CCK-8) for MRC5 and HFL1, which were treated with different concentrations of Hemin (80, 40 and 20 μM), also revealed modulation of radio-sensitization and protective effects in normal lung cells compared to Hemin-untreated cells (Figure 1d).

3.2. *Hemin induced radiosensitivity through ferroptosis in lung cancer cells*

In order to explore the effects of irradiation and Hemin on apoptosis and necroptosis, we treated the cells with Z-VAD-fmk (apoptosis inhibitor) and necrostatin-1s (necroptosis inhibitor), respectively. As shown in Fig. 2a, treatment with inhibitors did not restore the clonogenic survival in the cancer cells after irradiation and Hemin treatment. These results suggest that apoptosis or necroptosis is not involved in the irradiated cancer cells treated with Hemin.

Hemin has been reported to induce ferroptosis through overloading iron and initiating the Fenton reaction, in addition to its ability to degrade the proteins [40]. Therefore, we evaluated the impact of the ferroptosis inhibitor (ferrostatin-1, 5 μM) with clonogenic survival assay in A549 and H460 cells treated with 80 μM Hemin and fractionated IR doses (2 Gy/day) (Figure 2b and c). We found that ferrostatin-1 treatment restored the colony survival of cells treated with irradiation and Hemin. Interestingly, ferrostatin-1 restored colony survival of H460 cells after fractionated IR doses with or without Hemin treatment (Figure 2b), and this indicated that fractions of 2 Gy could only induce ferroptosis in these cells. In contrast, ferrostatin-1 failed to increase the colony survival of A549 cells treated with fractionated IR (Figure 2c), which indicated that 2 Gy/day did not trigger ferroptosis in A549 cells. Moreover, Hemin might cause substantial ferroptosis in A549 cells at 2 Gy/day since ferrostatin-1 completely restored colony survival after IR (Figure 2c). This finding was confirmed by treatment (Figure 2d) with another ferroptosis inhibitor, liproxstatin-1 (5 μM). The recovery of cell survival induced by liproxstatin-1 was similar to that induced by ferrostatin-1, implying that the Hemin-driven cell death in response to IR was ferroptosis.

Since the accumulation of lipid peroxidation was a defining feature of ferroptosis, C11-BODIPY was used to determine the amount of lipid peroxidation in our experiments. The results in Fig. 2e and f showed that treatment with Hemin (80 μM) substantially enhanced lipid peroxidation after radiation fractions of 3 × 2 Gy/day in A549 and H460 cells. The levels of oxidized C11-BODIPY were significantly reduced when the

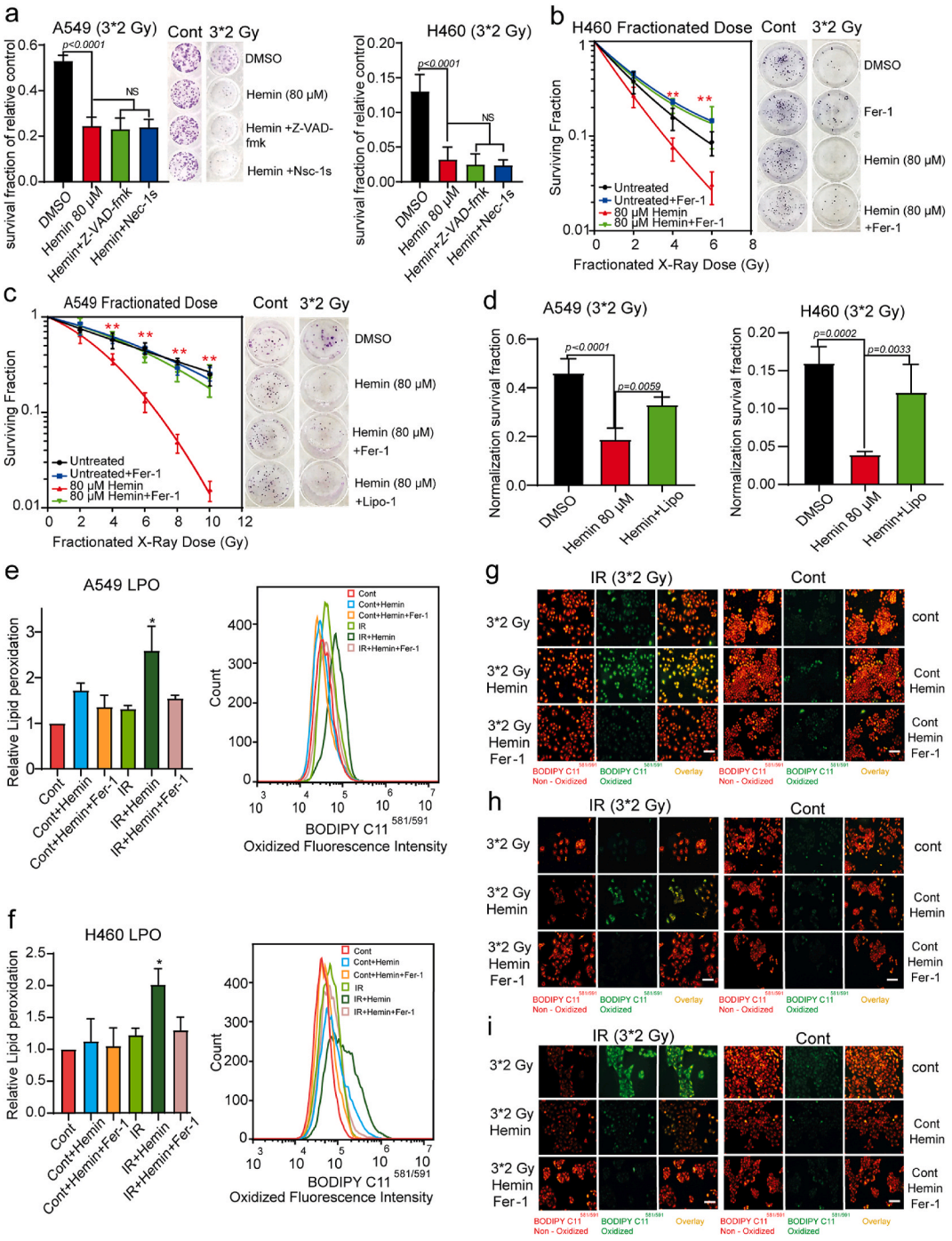

Fig. 2. Hemin induced radiosensitivity through enhancing ferroptosis. (**a**) Clonogenic survival of A549 and H460 cells treated with 80 μM Hemin and/or ZVAD-fmk/necrostatin-1 before irradiation (three fractions of 2 Gy/day). (**b**) and (**c**) Clonogenic survival curves of H460 and A549 cells treated with 80 μM Hemin and/or ferrostatin-1 (Fer-1) 2 h before irradiation (2 Gy/day). (**d**) Clonogenic survival of A549 and H460 cells treated with 80 μM Hemin and/or liproxstatin-1 2 h before irradiation (three fractions of 2 Gy/day). (**e**) and (**f**) Relative levels of lipid peroxidation (LPO) in A549 and H460 cells at 24 h after three fractions of 2 Gy/day. Error bars indicate ±SD and means from three independent repeats. *P*-values: * ≤ *0.05 &* ** ≤ *0.01*. (**g**) Fluorescent images of H460 (**h**) A549 (**i**) Beas-2B cells, stained with C11-BODIPY after treatment with 80 μM Hemin or combined with ferrostatin-1 for 2 h followed with fractionated doses (3 × 2 Gy/day).

irradiated cells were treated with a combination of 80 μM Hemin and 5 μM Ferrostatin-1. The expression of oxidized lipid peroxidation in H460 and A549 cells was also confirmed by the corresponding fluorescent images (Figure 2g and h). Surprisingly, the results in Fig. 2i showed a decreased amount of lipid peroxidation, indicating that Hemin protected Beas-2B cells from radiation-induced lipid peroxidation, which supported our findings on clonogenic formation in Fig. 1c and d.

3.3. Hemin reduced GPx4 expression in lung cells

We evaluated the involvement of Hemin in the reduction of GPx4 expression, which neutralized oxidized lipids and had been considered a hallmark of ferroptosis. As expected, there was a negative correlation between GPx4 expression and Hemin concentration (Figure 3a). Furthermore, both A549 and H460 cells showed increased HO-1 expression (Figure 3a). Based on this result, we studied whether

Hemin could reduce GPx4 expression in other lung cancer cell lines, including Calu-1 and H1299. We found that these cell lines were more sensitive to Hemin, and only 5–20 μM was enough to reduce GPx4 and increase lipid peroxidation (Figure S1 a, b, and c).

Since the primary function of GPx4 is to prevent ferroptosis, reduction of GPx4 levels will likely exacerbate lipid peroxidation and induce ferroptosis [13,41–44]. Fig. 3b represented GPx4 degradation with time in A59 and H460 cells following treatment with 80 μM Hemin. The expression of GPx4 was significantly decreased at 12 h and dramatically at almost 48 h. Furthermore, we investigated whether Hemin treatment affected GPx4 expression in normal lung cells such as Beas-2B, MRC5, and HFL1. The results (Figure 3c) showed that Hemin (80 μM) treatment significantly decreased GPx4 expression in MRC5 and HFL1 cells over time, but not in Beas-2B cells.

We investigated both the expressions of GPx4 and BACH1, since BACH1 worked as a heme sensor and had also been described as a regulator of heme oxygenase 1 and a nuclear transcription factor for several antioxidant proteins. We determined the BACH1 levels in lung cancer cells (A549 and H460) and normal lung cells (Beas-2B, MRC5, and HFL1) at different timepoints (1–48 h) after Hemin treatment. We found that BACH1 expression was downregulated within 1–6 h after treatment with Hemin (80 μM) (Figure 3b and c). The results showed that the expression level of BACH1 was marginally raised in 12 h and eventually returned to the control level in 24–48 h. There was an exception for Beas-2B cells, which showed a long-time degradation of BACH1 (48 h). On the other hand, as expected, HO-1 expression began to rise shortly after BACH1 degradation (Fig. 3) showing the regulation of BACH1 to HO-1, which agrees with the literature [19,20,45].

3.4. Regulation of GPx4 during radiation and Hemin modulated ferroptosis radiosensitivity

A significant trend of increased GPx4 expression following IR exposure was found in lung cancer cells (A549 and H460), as shown in Figures 4 a and b. We reasoned that IR-induced upregulation of GPx4 expression was most likely an adaptive response where the cancer cells

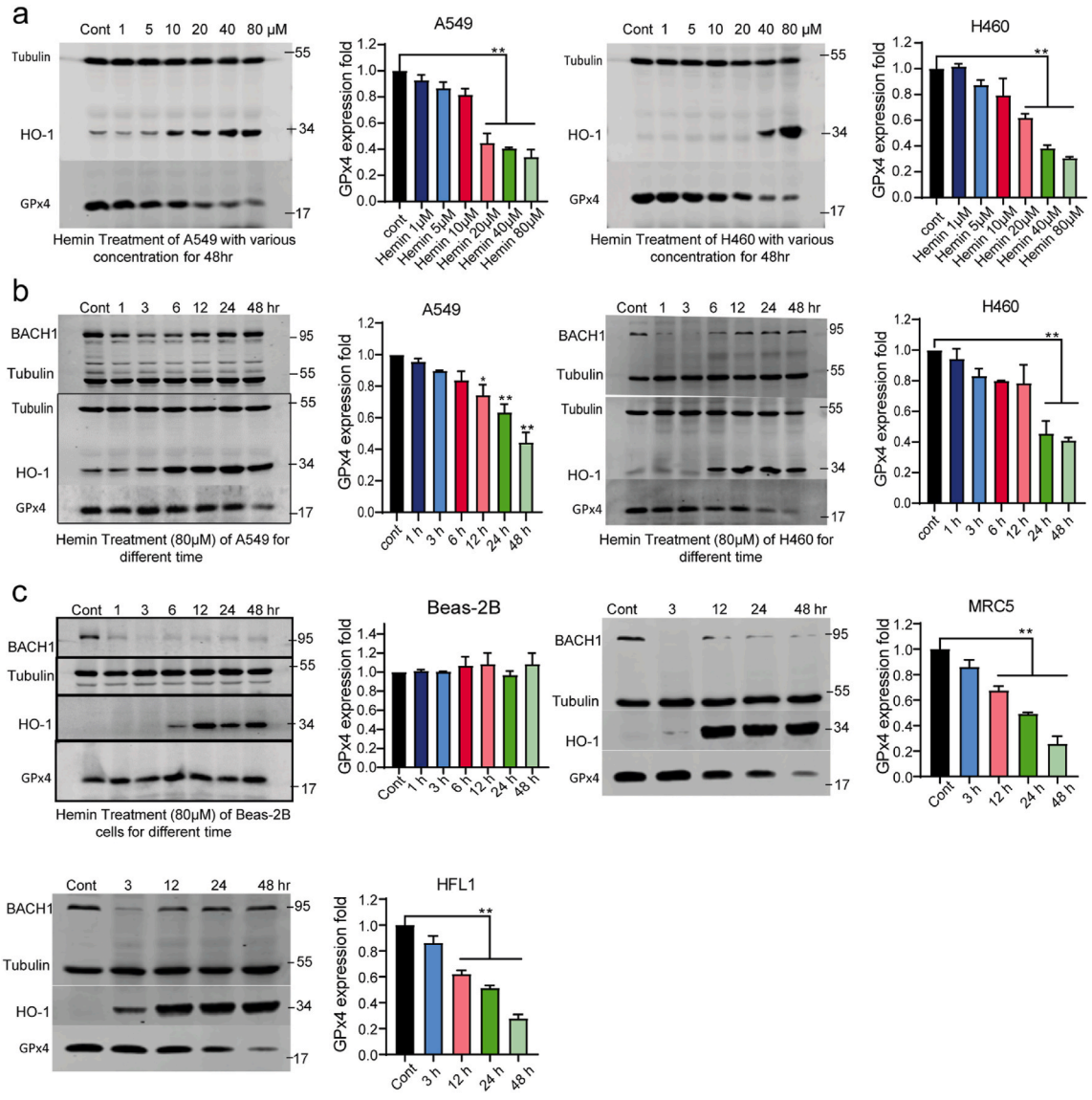

Fig. 3. Treatment of lung cancer and normal cells with Hemin decreased GPx4. (**a**) Western blot analysis of HO-1 and GPx4 expressions at 48 h in A549 and H460 cell lines for various Hemin concentrations (0–80 μM). (**b**) Western blotting of BACH1, HO-1 and GPx4 expressions in A549 and H460 cell lines treated with 0 μM (cont) and 80 μM Hemin for different time (1–48 h). (**c**) Western blot analysis of BACH1, HO-1 and GPx4 expression in normal lung cells (BEAS-2B, MRC5 and HFL1 cell lines) treated with 0 μM (cont) and 80 μM Hemin for different time (1–48 h). Error bars are means ± SD, n = 3 independent repeats. *P-values* were calculated using one-way ANOVA. *P*-values: * ≤ *0.05* & ** ≤ *0.01*.

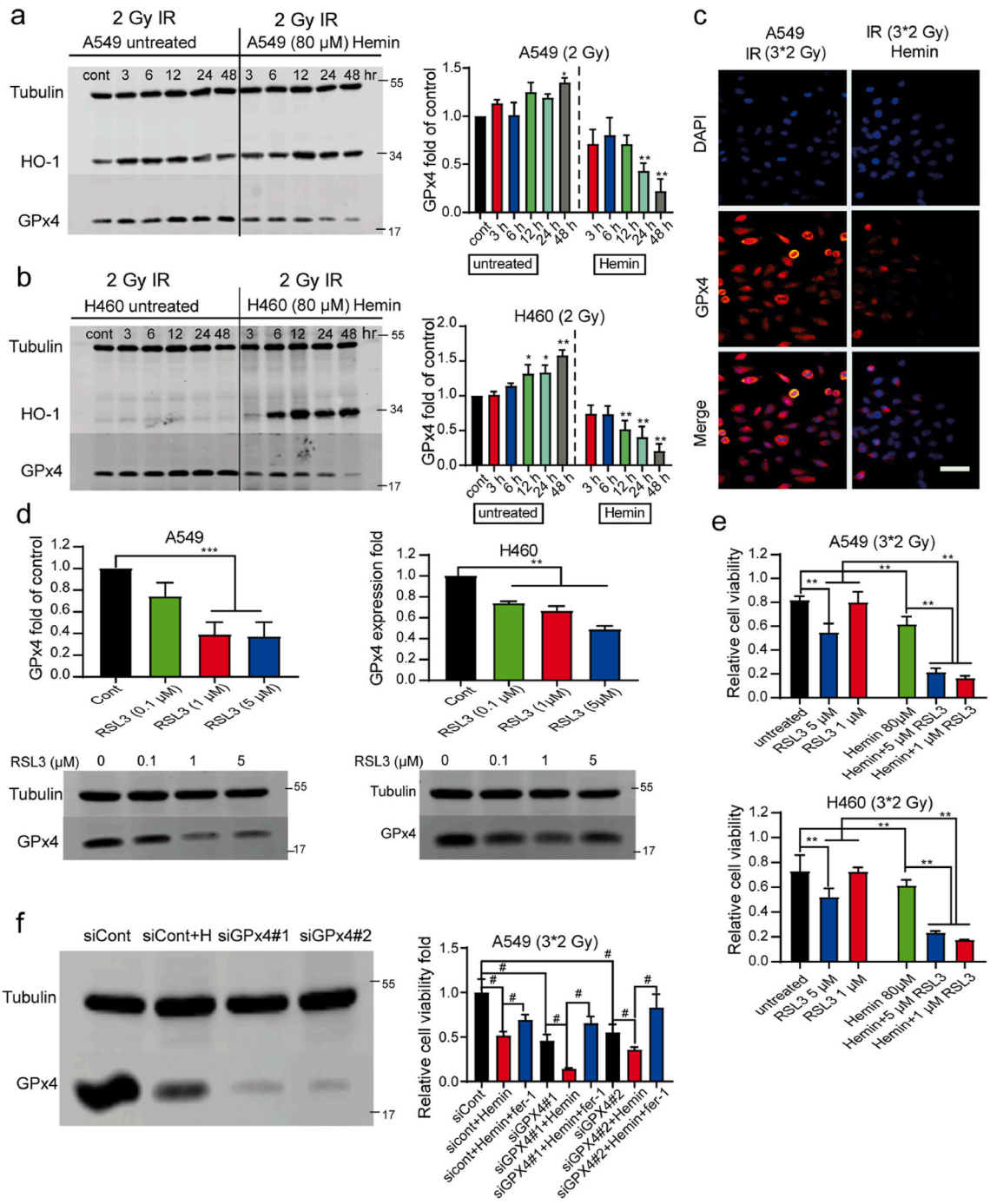

Fig. 4. Radiation-induced elevation of GPx4 expression and its role in modulating ferroptosis radiosensitivity. (**a**) and (**b**) Western blot analysis of HO-1 and GPx4 expression at different timepoints of irradiation (2 Gy) for A549 and H460 cells treated with or without 80 μM Hemin (1–48 h). (**c**) Immunofluorescence of GPx4 in A549 cells irradiated with dose fractions (3 × 2 Gy) with or without treatment with 80 μM Hemin. (**d**) Western blot analysis of GPx4 expression in A549 and H460 cells at 48 h after treatment with RSL3. (**e**) Cell viability (48 h post IR) after treatment with RSL3 (0, 1 and 5 μM) or combined with 80 μM Hemin followed with fractionated 3 × 2 Gy irradiation. (**f**) Cell viability (48 h post IR) after transfection of the negative control (siCont) or two siRNAs (siGPx4#1 and #2). A549 cells (4 × 10^3) treated with 80 μM Hemin and 3 × 2 Gy irradiation. SD was shown by the error bars. *P*-values, *# or * ≤ 0.05 & **≤0.01.*

attempted to deal with the stress from IR and thus enhance cell survival, which might contribute to radioresistance [7,8,11]. After 24–48 h, treatment with 80 μM Hemin significantly reduced the upregulation of GPx4 induced by IR, as shown in Fig. 4a and b. This finding was verified by the immunofluorescence of the GPx4 in response to IR and Hemin (Figure 4c).

IR-induced expression of GPx4 and high levels of GPx4 might contribute to radioresistance [6,8,11,46]. Since GPx4 inhibits ferroptosis through decreasing the complex of phospholipid hydroperoxides, IR-induced GPX4 expression will probably play a role in IR-induced ferroptosis. Therefore, we decided to investigate if inactivating GPx4 with the RAS-selective lethal (RSL3) inhibitor might enhance IR sensitization of cancer cells. Our results showed that expression of GPx4 was reduced in both A549 and H460 cells after RSL3 treatment (Fig. 4d). Moreover, we investigated how RSL3 treatment affected the radiosensitivity of A549 and H460 cells. We used RSL3 to pre-treat cancer cells for 12 h before exposing to fractioned radiation (3 × 2 Gy). We found that combining IR with RSL3 treatment resulted in synergistic increases

in cell mortality in the examined cancer cells (Fig. 4e). As expected, our results showed significant cell death with 5 μM RSL3 treatment, whereas a lower concentration (1 μM) failed to improve IR sensitivity. Surprisingly, when we coupled RSL3 with Hemin, we detected significantly more cell mortality for both dosages of RSL3 (5 and 1 μM) when compared with no Hemin treatment (Figure 4e). This finding indicated that IR sensitization with Hemin was not simply connected to GPx4 inhibition. We hypothesized iron overload as another possible factor that caused Hemin ferroptosis.

For further verification, siRNAs were applied to inhibit GPx4 expression in A549 cells. After two days of 3 × 2 Gy, the radiosensitivities of the GPx4-knockdown cells (siGPx4) and control cells (siCont) were determined with CCK-8 test. As regards A549 cells, siGPx4 cells had higher radiosensitivity than siCont cells (Fig. 4f). When the cells with GPx4 knockdown were treated with Hemin, severe mortality was detected after 3 × 2 Gy, which was similar to our previous results on the effect of RSL3. Ferrostatin-1 (5 μM) could partially prevent GPx4-inhibition-induced cell death (Fig. 4f), indicating that GPx4 inhibition caused ferroptosis to sensitizing lung cancer cells, which agreed with the literature [41–43].

Based on the results shown in Fig. 4, we postulated that the decrease in GPx4 observed in Hemin-treated cells might impair antioxidant defense and played a role in radiosensitization. The results from CCK-8 test in Fig. 4 e and f showed a less sensitizing impact of Hemin than the results from colony formation assay (Figs. 1 and 2). The discrepancy was attributed to differences in the mechanisms and the sensitivity of

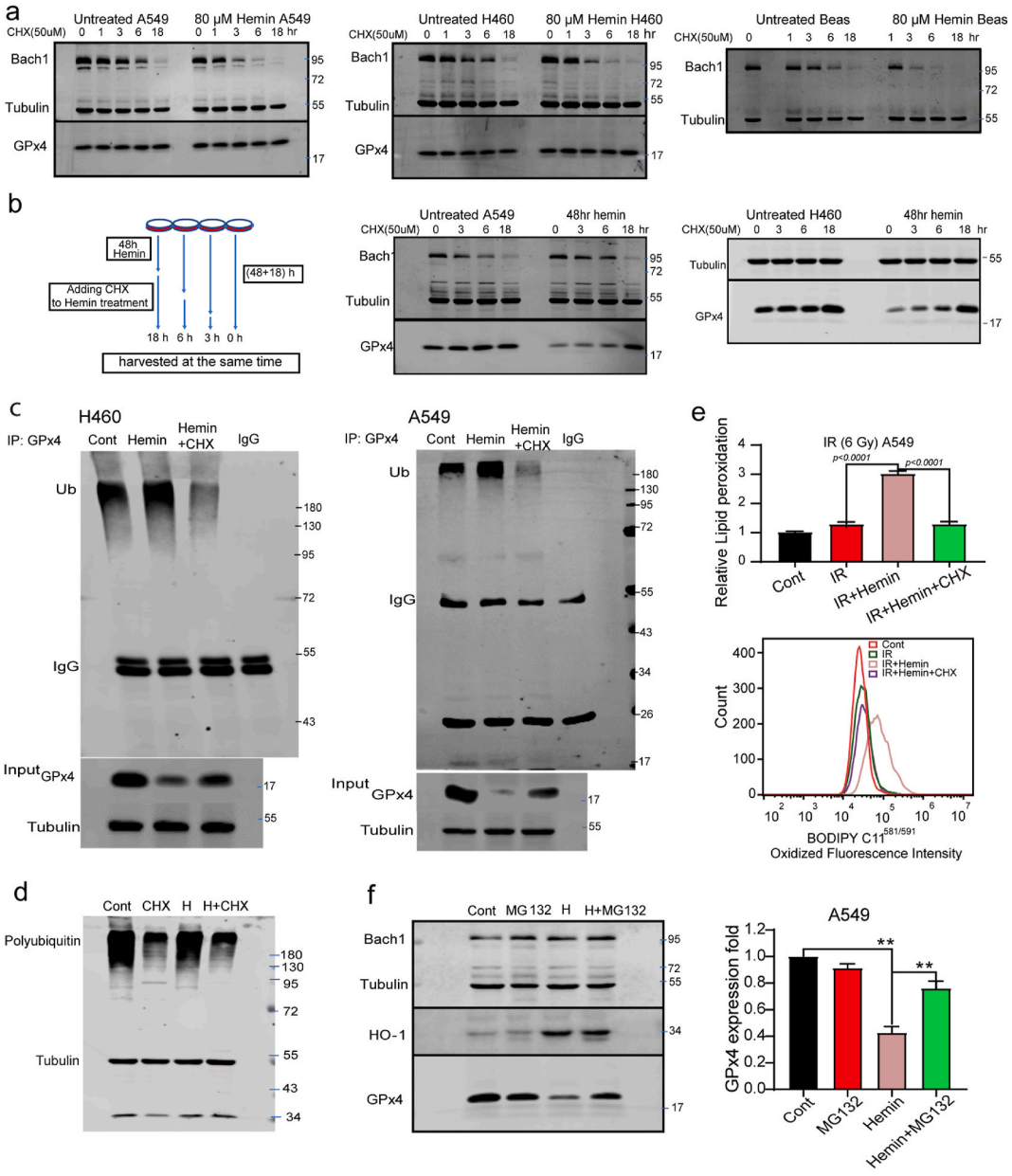

Fig. 5. Hemin induced degradation of BACH1 and GPx4 ubiquitination. (**a**) BACH1 and GPx4 levels in A549, H460 and Beas-2B cells after treated with or without Hemin (80 μM) combined with 50 μM CHX at different time intervals. (**b**) BACH1 and GPx4 levels in A549 and H460 cells treated with or without 80 μM Hemin treatment for 48 h and followed by additional 3–18 h treatment of 50 μM CHX. (**c**) Immunoprecipitation of GPx4 after treatment with or without Hemin for 48 h followed by 18 h CHX treatment in A549 and H460 cells. (**d**) Total polyubiquitin level in A549 cells Hemin (80 μM) combined with 50 μM CHX for 18 h. (**e**) Lipid peroxidation (LPO) levels in A549 cells after 48 h treatment of Hemin followed by CHX treatment and IR exposure (6 Gy). Error bars are ±SD around means and calculated from three independent repeats. (**f**) BACH1, HO-1 and GPx4 levels in A549 cells at (48 + 18) h after treatment with 80 μM Hemin (H) followed by treatment with 10 μM MG123 for additional 18 h (48 h Hemin +18 h CHX), and the cells were harvested at the same time. *P-value,* * ≤ *0.05 &* **≤*0.01.*

detection techniques and also in part due to different cell densities, confluence and Hemin treatment.

3.5. Hemin induced ubiquitination and degradation of GPx4

In order to study how Hemin induces downregulation of GPx4, we investigated the mRNA levels of GPx4 and HO-1. According to our results (Figure S2 a), Hemin did not influence GPx4 transcription, but as we expected, Hemin treatment significantly upregulated HO-1 at the mRNA level.

Furthermore, to determine if Hemin was involved in the degradation of GPx4 in addition to BACH1 as a sensor of heme, we detected GPx4 and BACH1 expression levels at specific timepoints upon treatment with 50 μM cycloheximide (CHX), a protein translation inhibitor, in the presence or absence of Hemin. Hemin dramatically increased the rate of degradation of endogenous BACH1 compared to Hemin-untreated cells, indicating that BACH1 degraded quickly in the presence of Hemin (Fig. 5a). Surprisingly, we found that lung cancer cells (A549 and H460) and normal cells (Beas-2B) had full GPx4 stabilization at early timepoints (max to 18 h) upon Hemin treatment (Figure 5a).

Considering that Hemin has a late effect in downregulating GPx4, we treated the cells with Hemin for 48 h before 50 μM CHX treatment for a maximum of an additional 18 h to inhibit protein translation synthesis. Interestingly and unexpectedly, the results in Fig. 5 b showed that the expression of GPx4 was considerably increased after Hemin-induced degradation in the presence of CHX. This observation suggested that Hemin might indirectly degrade GPx4, which depended on other regulator-proteins and was affected by CHX. It was suggested that CHX might have a role in downregulating ubiquitination mechanisms. To confirm and assess the efficiency of CHX, HO-1 protein expression was measured. We observed that the expression of HO-1 was reduced in the presence of CHX (supplementary S2 b), while a 15-fold increase in HO-1 mRNA as found in CHX-Hemin treated cells (supplementary S2 a).

Since polyubiquitination is one part of the proteasome-dependent degradation of proteins, we investigated whether Hemin increased GPx4 ubiquitination. After treatment with Hemin for 48 h and/or followed by adding CHX for an additional 18 h, all groups of A549 and H460 cells were harvested and treated with GPx4 antibody. Fig. 5 c showed that Hemin promoted GPx4 ubiquitination. The percentages of detectable ubiquitinated GPx4 in Hemin-treated A549 or H460 cells were slightly higher than those in untreated cells. As soon as a polyubiquitin-tagged target protein (GPx4) is identified, it is directed to the proteasome for degradation [39,47]. Therefore, the ubiquitinated GPx4 amount, which was considered as a rate at the time of detection, was slightly increased with Hemin treatment. Thus, because GPx4 degradation in response to Hemin treatment took a long time, i.e., (48 + 18) hours, the total amount of GPx4 was significantly decreased (Fig. 5c).

Furthermore, we found that CHX effectively inhibited GPx4 ubiquitination (Figure. 5c), indicating that CHX disrupted GPx4 ubiquitination and led to a reduction in the degradation process in Hemin treatment to cause increased GPx4 expression. To study the effect of CHX on ubiquitination, the total polyubiquitin proteins were blotted after 48 h treatment with or without Hemin followed by an additional 18 h treatment with CHX. We found that CHX reduced the total ubiquitination as shown in Fig. 5 d.

We further investigated the possible activity of GPx4 which was increased in the presence of CHX. Flow cytometry analysis of lipid peroxidation (LPO) with a particular fluorescent probe (C11-BODIPY) revealed a substantially decreased level, suggesting the increased activity of GPx4 (Figure 5e).

Finally, we tested whether a proteasome inhibitor (MG123) could successfully prevent GPx4 degradation in response to Hemin exposure. As shown in Fig. 5 f, pretreatment of A549 cells with Hemin for 48 h followed by an additional 18 h treatment with MG123 (10 μM) decreased GPx4 degradation, indicating that GPx4 degradation was controlled by the proteasome.

3.6. FTH1 protected normal lung cells from radiosensitization of Hemin

Our results in Fig. 4 showed that Hemin drastically enhanced the effect of RSL3, or siRNA against GPX4 on irradiated cells, which indicated that Hemin had further contributions to changes in radiosensitivity. It is suggested that free iron overload, as a byproduct of Hemin degradation, plays a critical role in this lung-cancer death. As regards the different responses between cancer and normal lung cells to radiosensitization by Hemin, we hypothesized different iron thresholds and hemostasis pathways in cancer and normal cells due to the difference in metabolism and stress adaptation.

FTH1 is a major protein storing iron in a soluble and harmless form via converting Fe^{2+} to Fe^{3+} to avoid oxidative damages caused by Fenton reactions, particularly to the cell membrane. As shown in Fig. 6a, a slightly elevated level of FTH1 at 12 h after Hemin treatment was observed in A549 and H460 cells. This response of FTH1 rapidly diminished over time in lung cancer cells, whereas normal lung cells (Beas-2B, MRC5 and HFL1) had extremely high FTH1 expression following Hemin treatment (80 μM). Unlike cancer cells, this large amount of FTH1 was stable over time in normal lung cells (Figure 6a). In response to Hemin, FTH1 expressions in normal lung cells were approximately 10–15 times higher than those in lung cancer cells (Figure 6b). FTH1 selectively oxidizes ferrous iron and tightly regulates the labile prooxidant iron pool homeostasis [32,34,35]. To maintain the cellular iron and ROS redox balance, the FTH1 molecule can chelate up to 4500 iron atoms [30].

To determine the regulatory role of FTH1 in radiosensitivity, we next investigated the cytoprotective effect of high expression of FTH1 and its important activity under high-dose Hemin treatment to prevent iron from triggering ferroptosis in normal lung cells. We knocked down FTH1 in Beas-2B and MRC5 cells with siRNA interference (Figure 6c). Following transfection, the cells were treated with Hemin and irradiated with 3 × 2 Gy/day and incubated for an additional two days after the final IR. The results of cell viability revealed that FTH1 knockdown in irradiated cells reduced the survival of normal lung cells after Hemin treatment, indicating that the cells became more sensitive to IR (Figure 6c), which was the opposite to the protection role of Hemin shown in Fig. 1d. The most likely explanation was that the knockdown of FTH1 increased intracellular iron availability, which led to an increase in ROS exceeding the antioxidant threshold and thereby increasing cell death in response to IR. Our results strongly suggested that the antioxidant properties of FTH1 played a critical role in determining the ROS level in response to Hemin and in triggering ferroptosis.

3.7. Hemin "amplified" ROS induced by IR in lung cancer cells

To assess the influence of Hemin pretreatment for 48 h on early ROS generation following 2 Gy IR, the cells were treated with DCFH-DA substrate and subsequently irradiated. Our results in Fig. 7 showed that Hemin or iron, as a Hemin breakdown product, increased the initial ROS induction following IR. As demonstrated in Fig. 7 a and b, the cells treated with Hemin showed a high level of ROS, roughly 70-fold and 8-fold in A549 and H460, respectively. These findings were consistent with those of the clonogenic assay and lipid peroxidation. We found that Hemin treatment in H460 cells had a lower potential to "amplify" ROS than in A549 cells (Figure 7a and b), which was most likely due to the relatively high FTH1 level in H460 cells at 48 h after Hemin treatment (Figure 6b).

Furthermore, we found an increase in ROS production in Hemin-treated cells after 3 days of IR, as shown in Supplementary information (Figure S2 c and d), which was attributed to byproducts of cellular respiration in mitochondrial damages caused by irradiation-induced stress [48]. An unexpected finding was that Hemin treatment reduced initial ROS generation in irradiated normal lung cells such as Beas-2B

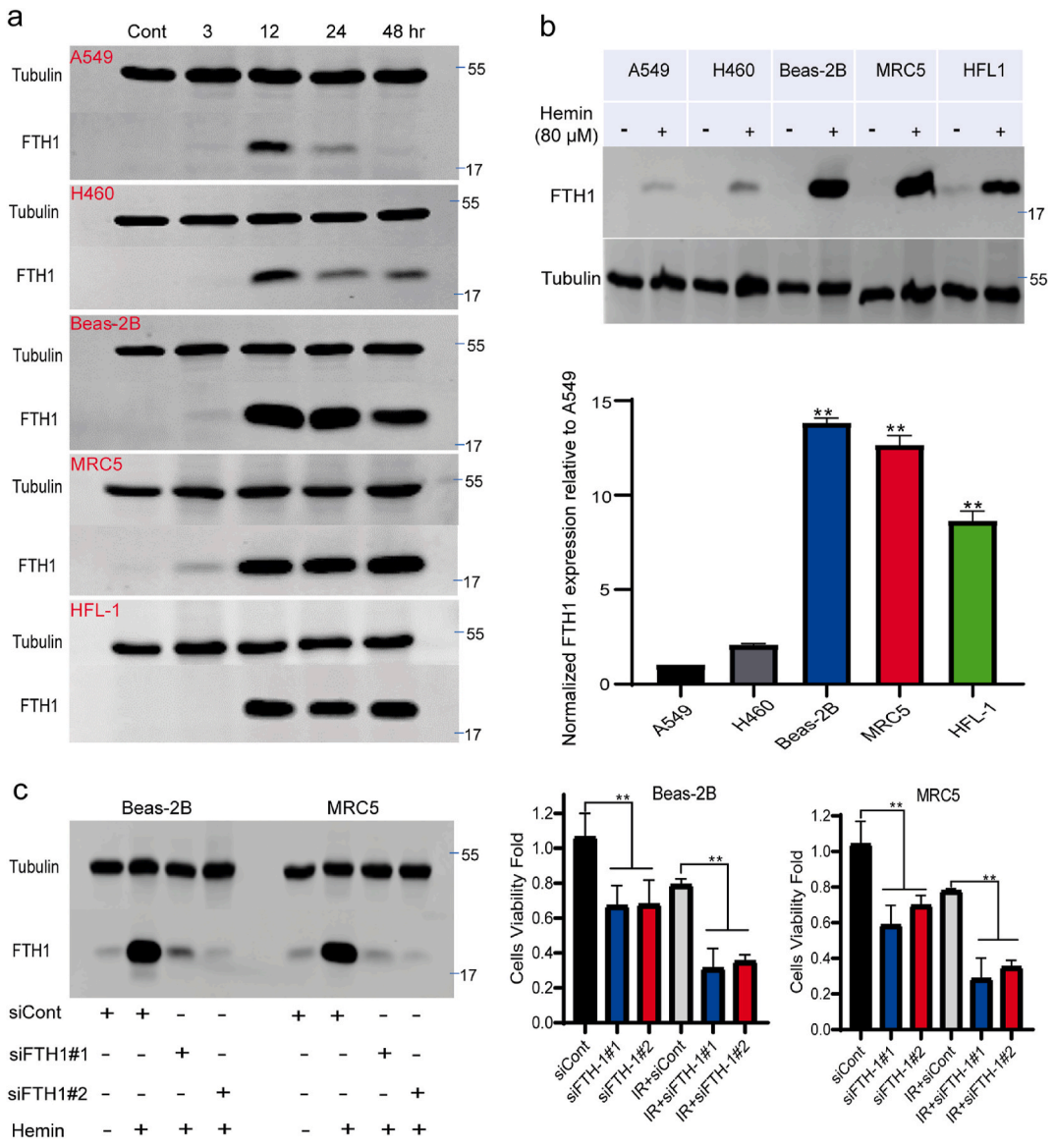

Fig. 6. FTH1 protected normal lung cells from Hemin sensitization to IR. (a) FTH1 levels in lung cancer cells (A549 and H460) and normal lung cells (Beas-2B, MRC5 and HFL1) treated with 80 μM Hemin at different time points. (**b**) Comparison of FTH1 levels at 48 h in lung normal and cancer cells treated with 80 μM Hemin. (**c**) Western blot analysis for FTH1 knockdown with siRNA interference in Beas-2B and MRC5 cells treated with 80 μM Hemin for 48 h, and cell viability after combined treatment with Hemin and IR exposure to 3 × 2 Gy. Error bars are ±SD around means and calculated from three independent repeats. *P*-values, $* \leq 0.05$ & $** \leq 0.01$.

cells (Figure 7c). We proposed that this reduction in ROS might play a role in enhancing cell survival.

Moreover, Bilirubin is another metabolic end product of Hemin and has been identified as a strong antioxidant. Therefore, we further examined the kinetics of Bilirubin production after treating A549 and Beas-2B cells with Hemin (80 μM) for 48 h followed by 2 Gy IR. The cells were harvested immediately, and 500 μg of lysate was employed for Bilirubin analysis. As shown in Fig. 7 d and Fig. S2 e, there was a substantial difference in the kinetic production of Bilirubin in Hemin-treated Beas-2B cells compared to untreated Beas-2B cells after IR, but no such difference was observed in A549 cells. It is remarked that Bilirubin is produced from Biliverdin by Biliverdin reductase BVR [36–38].

Since we did not detect significant changes in Bilirubin in A549 cells treated with Hemin, we investigated the effect of bilirubin on ROS in irradiated A549 cells with or without Hemin. Therefore, we added exogenous bilirubin (1 μM) within the physiological range [49]. We observed that exogenous Bilirubin played a role in decreasing ROS produced by the combined treatment with Hemin and IR, but it did not eliminate the ROS produced by irradiation alone (Fig. 7 e1 and 2). This suggests that bilirubin can remove specific ROS, most likely the lipophilic ROS produced by the Fenton reaction causing ferroptosis [36–38].

3.8. Hemin enhanced IR-induced tumor suppression in vivo

Finally, we performed an *in vivo* study to investigate the effect of Hemin on shrinking tumors by fractioned irradiation, with the experimental design shown in Fig. 8a. We treated mice with two intratumoral injections of Hemin (20 mg/kg) or the same volume of PBS, followed by three fractioned IR of 2 Gy/12 h in the tumor area in nude mice (Figure 8b). After 14 days, the control mice that were injected with Hemin had no effect on the tumor development of A549 xenografts, but the combined treatment of Hemin and fractionated IR (6 × 2 Gy/12 h) substantially sensitized and inhibited xenograft tumor growth in nude mice (Figures 8c and d). Moreover, our research indicated that six fractionated doses of 2 Gy/12 h did not significantly reduce the development of A549 xenograft tumors after 14 d. However, statistical analysis revealed a substantial reduction in tumor weights by fractionated doses of 6 × 2 Gy/12 h, and by the combined treatment with Hemin

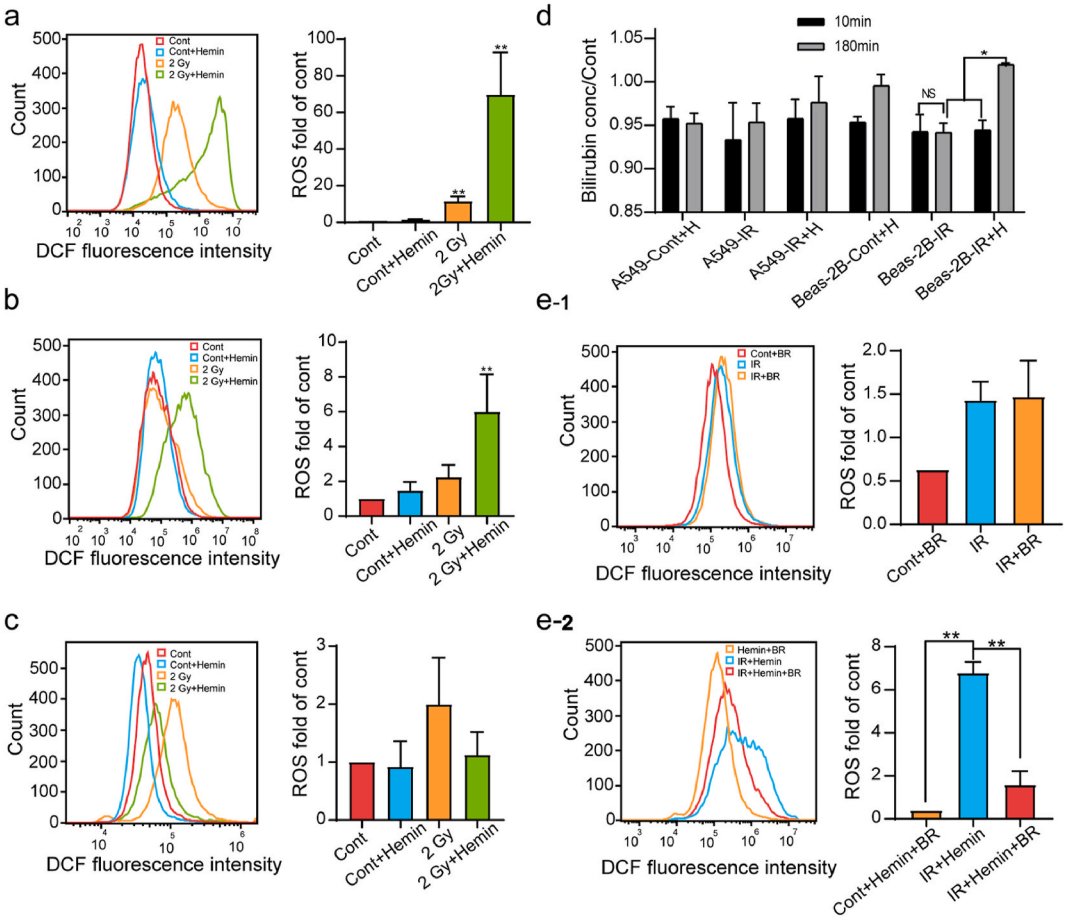

Fig. 7. Effect of Hemin and Bilirubin (BR) on initial ROS generation after IR. (**a**), (**b**) and (**c**) Flow cytometry of DCF fluorescence of A549, H460 and Beas-2B cells treated for 48 h with 80 μM Hemin followed by 10 μM of DCFH at 10 min before IR exposure. (**d**) Colorimetric measurement of Bilirubin fold in irradiated (2 Gy) A549 and Beas-2B cells with or without treatment with 80 μM (H) Hemin for 48 h. (**e**) Flow cytometry of DCF fluorescence of A549 cells after treatment with 1 μM Bilirubin (BR) at 30 min before IR (2 Gy). *P*-values, * ≤ *0.05* & ** ≤ *0.01*.

and fractionated radiation (Figure 8f). Although we noticed weakness in both irradiated nude mice treated with Hemin or PBS, we did not observe a substantial decrease in their body weights (Figure 8e).

4. Discussion and conclusions

Previous research found that IR promoted ferroptosis via inducing lipid peroxidation, which enhanced the removal of electrons from PUFAs to generate fatty-acid radicals [11]. In this study, we investigated the role of Hemin as an iron overloading agent capable of generating ROS via the Fenton, Fenton-like, and Haber-Weiss reactions, which were activated by the initial free radical and hydrogen peroxide produced by IR [26]. Iron is necessary for the aggregation of lipid peroxides and the induction of ferroptosis. Therefore, ferroptosis sensitivity is affected by iron overload, export, and storage [17,25,40]. On the other hand, Hemin degradation produces Biliverdin, which might be converted to Bilirubin with cytoprotective properties [36–38]. We found different functions of Hemin in lung cancer cells and non-cancer cells. The most important and fascinating result was the enhancement of ferroptosis and radiosensitivity in lung cancer cells by Hemin, and at the same time the protection of non-cancer cells (Beas-2B, MRC5 and HFL1). This distinct difference indicates the possible use of Hemin in cancer radiotherapy via selectively destroying cancer cells while protecting non-cancer cells.

We demonstrated that Hemin increased ferroptosis in lung cancer cells, notably in lung cancer cells irradiated with fractionated doses (Fig. 1). With mechanistic studies summarized in Scheme 1, Hemin causes lipid peroxidation, a hallmark of ferroptosis, when lung cancer cells are exposed to fractionated doses (3 × 2 Gy) (Fig. 2). As shown in Fig. 7 a and b, Hemin exacerbated the generation of ROS, which might reach up to 70-fold in A549 cells after 2 Gy IR. As a result, we proposed that Hemin or certain free iron increased ROS via Fenton and Haber-Weiss reactions. Thus, ROS attacked the cell membrane and led to lipid peroxidation accumulation and the induction of ferroptosis. Consequently, we found a significant increase in lipid peroxidation, especially in lung cancer cells treated with the combined treatment with Hemin and radiation (Fig. 2).

Interestingly, we found that the malignant lung cells “attempted” to protect themselves from lipid peroxidation via overexpressing GPx4 to increase radioresistance (Fig. 4), which was consistent with results from previous studies [8,11]. We also found that Hemin increased the rate of GPx4 ubiquitination and degraded it over time, in contrast to previous results for primary cortical neurons [17]. Therefore, the decrease in GPx4 expression due to Hemin treatment weakened the defense for lung cells. Although RSL3 and siGPx4 enhanced the radiosensitivity of lung cells, significant death of lung cancer cells would result upon combined with Hemin (Figure 4e).

Ferritin is the most common molecule involved in iron homeostasis in biology, and its primary function is to oxidize and bind Fe^{2+}, as well as to regulate iron storage and availability [29,31,32,34,50]. When we treated lung cancer cells with 80 μM of Hemin, we found no indication of an adequate increase in the expression of iron storage protein (FTH1) to protect the cells from excess iron (Fig. 6). Furthermore, as Hemin degradation produced Biliverdin, we found no increase in the kinetic production of Bilirubin in A549 lung cancer cells, which offered

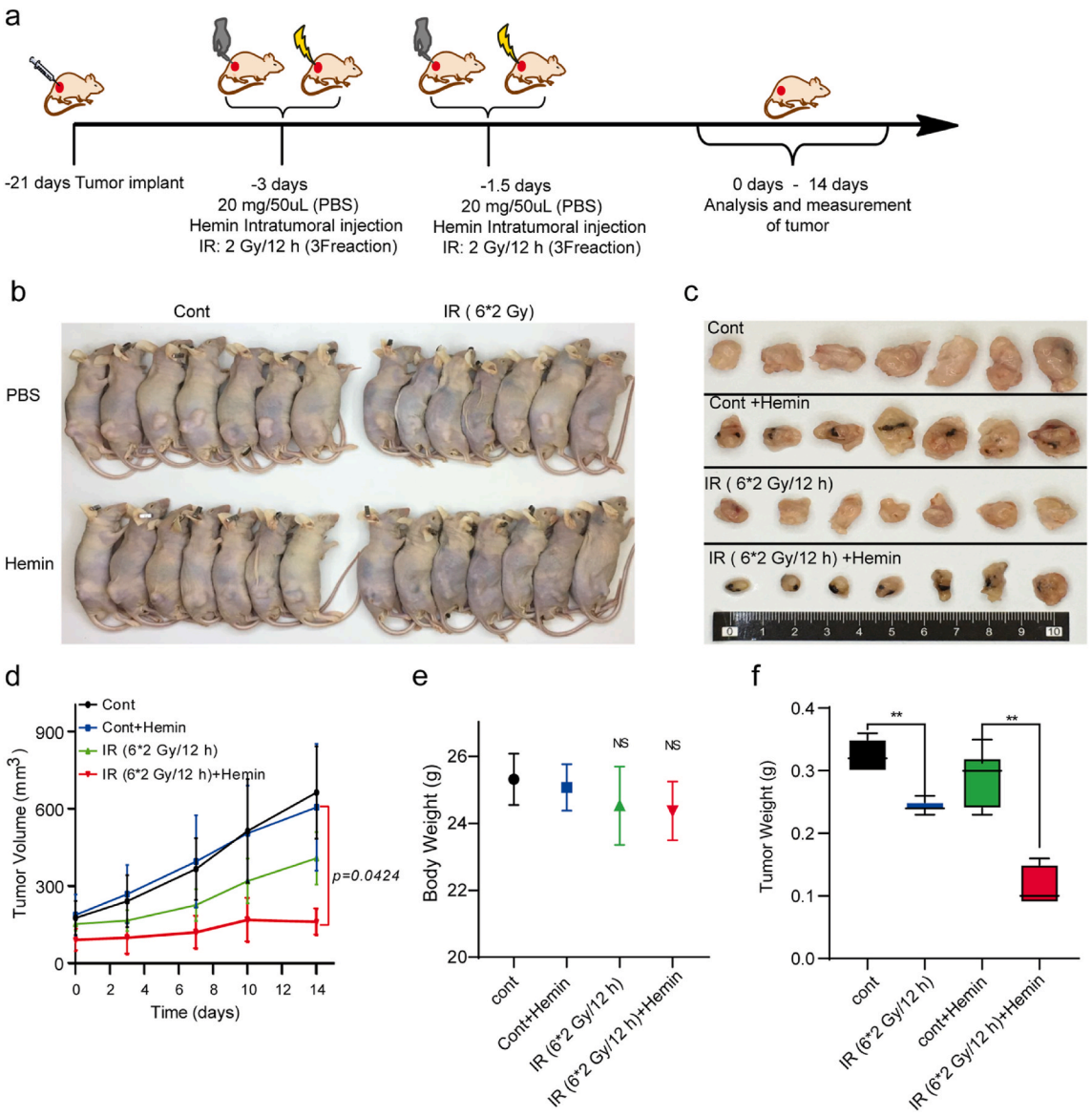

Fig. 8. Hemin enhanced IR-induced tumor suppression *in vivo*. (**a**) Schematic of experimental design for xenograft tumors treated with two intratumoral injection of Hemin (20 mg/kg) or the same volume of PBS followed with three fractions of 2 Gy/12 h in nude mice. (**b**) Images of nude mice at 14 d after treatment with two intratumoral injections of Hemin followed with three fractions IR of 2 Gy/12 h. (**c**) Representative images of A549 tumors (**d**) Volumes of A549 xenograft tumors at different timepoints (d). (**e**) Body weights of nude mice at 14 d post IR. (**f**) Weights of xenografts at 14 d post IR. Error bars are ±SD around means, n = 7. *P* values were determined with one-way ANOVA. * ≤ *0.05* & ** ≤ *0.01*.

cytoprotection against ROS (Fig. 7) [36–38]. Therefore, the failure in the induction of FTH1 and Bilirubin together increased the stress in irradiated lung cancer cells.

Our findings indicated that intratumoral Hemin injection sensitized the lung cancer xenograft to fractionated IR *in vivo* (Fig. 8). Moreover, the results from many lung cancer cell lines supported the proposed combined treatment approach. Remarkably, when Calu-1 and H1299 cells were exposed to IR, these cells were more sensitive to Hemin-induced ferroptosis (S1 a, b, and c). According to the Food and Drug Administration (FDA), Hemin for injection is a drug frequently used to treat acute intermittent porphyria (AIP). Therefore, our findings may encourage future investigation on the combined treatment with Hemin and ionizing radiation.

On the other hand, Hemin protected non-cancer lung cells (normal lung cells) from IR-induced cell death (Fig. 1). For normal lung cells, Hemin increased the expression of the ferrous storage protein FTH1 (Fig. 6), which might reduce the Fenton reaction and subsequently suppressed lipid peroxidation [29,51]. Therefore, FTH1 neutralized the effects of iron overloads produced from Hemin degradation. Moreover, the kinetic synthesis of Bilirubin was shown as an additional mechanism in protecting irradiated normal lung cells treated with Hemin (Figure 7d). Our findings showed that Bilirubin played a role in reducing ROS produced by Hemin in irradiated cells (Figure 7e). Previous research revealed that when Bilirubin interacted with lipophilic ROS, it was oxidized to Biliverdin and then converted to Bilirubin by BVR (Biliverdin-Bilirubin cycle) [36–38]. We suggested that the decrease of GPx4 in normal cells was not sufficient to interrupt the antioxidant to induce cell killing, especially under strong expression of FTH1 and elevation of Bilirubin, which might substitute the antioxidant function of GPx4. It would be pertinent to further explore the role of Bilirubin as a lipophilic ROS scavenger and a ferroptosis inhibitor, and the detailed mechanism of how FTH1 expression differed in cancer and normal lung cells in response to Hemin.

In summary, the findings of this study demonstrated that Hemin

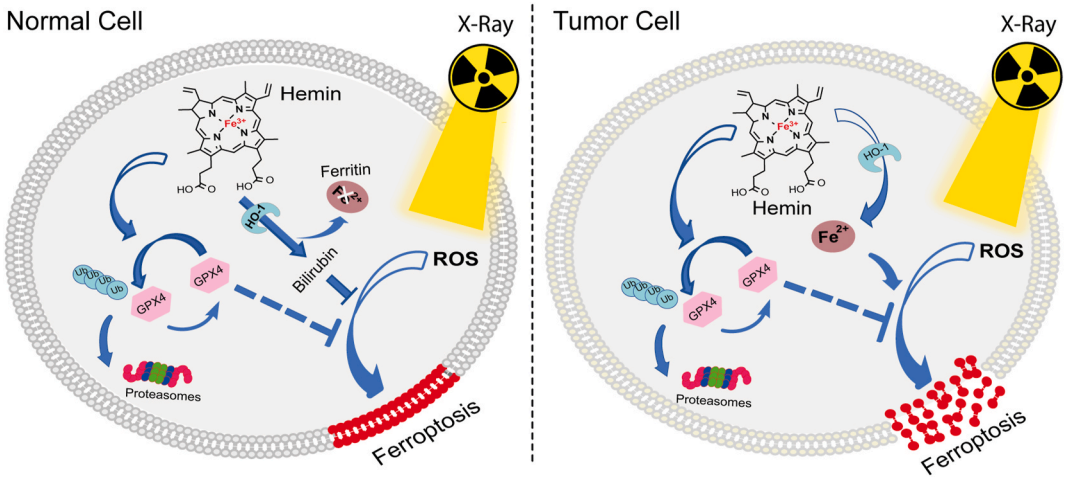

Scheme 1. Dual roles of Hemin inducing/inhibiting ferroptosis in lung cancer/non-cancer cells. In the presence of Hemin substrate, HO-1 is upregulated, leading to release of Fe^{2+} to participate in the Fenton reaction in irradiated cancer lung cells and triggering ferroptosis death. In normal lung cells, elevation of FTH1 stores the released iron from Hemin degradation, and Bilirubin might play a role as an antioxidant. Hemin also enhanced the GPx4 ubiquitin-proteasome system (UPS).

might cause ferroptosis in lung cancer cells when exposed to fractioned doses of IR but also protected normal lung cells. Our findings highlighted that Hemin could induce GPx4 degradation. In addition, we showed that Hemin induced significant FTH1 expression to store more iron in normal lung cells than in cancer cells. Comprehensive *in vivo* studies are needed to further assess the use of Hemin in association with ionizing radiation in treating cancers.

Author contributions

Conceptualization, Waleed. A. Almahi and Wei Han; methodology, Waleed. A. Almahi and P.K.; software, Waleed. A. Almahi; validation, Waleed. A. Almahi, P.K., K.N.Y., F.A. and W.H.; formal analysis, Waleed. A. Almahi; investigation, Waleed. A. Almahi; resources, Waleed. A. Almahi; data curation, Waleed. A. Almahi and F.M.; writing original draft preparation, Waleed. A. Almahi and K.N.Y.; writing review and editing, K.N.Y. and W.H.; visualization, Waleed. A. Almahi; supervision, W.H.; project administration, W.H.; funding acquisition, W.H. All authors have read and agreed to the published version of the manuscript without Conflicts of Interest.

Funding

This research was supported by the Chinese National Natural Science Foundation of China (grant no. 81974484), CASHIPS Director's Fund (grant no. YZJJ2018QN19) and project funded by the Priority Academic Program Development of Jiangsu Higher Education Institutions (PAPD) and Jiangsu Provincial Key Laboratory of Radiation Medicine and Protection. This research was also supported by the research grant IRF/0024 from the State Key Lab in Marine Pollution (SKLMP), City University of Hong Kong.

Institutional review board statement

All animal studies were conducted according to protocols approved by the Ethical Committee of Experimental Animals of Hefei Institutes of Physical Science, Chinese Academy of Sciences.

Acknowledgment

We gratefully acknowledge financial support for the Ph.D. scholarship programme from CSC as well as Sudan Atomic Energy Commission fellowship mission help.

Appendix A. Supplementary data

Supplementary data to this article can be found online at https://doi.org/10.1016/j.yexcr.2021.112946.

References

[1] J.A. Barta, C.A. Powell, J.P. Wisnivesky, Global epidemiology of lung cancer, Ann. Glob. Heal. 85 (1) (2019) 1–16, https://doi.org/10.5334/aogh.2419.
[2] T. Oike, T. Ohno, Molecular mechanisms underlying radioresistance: data compiled from isogenic cell experiments, Ann. Transl. Med. 8 (6) (2020), https://doi.org/10.21037/atm.2020.02.90, 273–273.
[3] C. Veiga, et al., Investigation of the evolution of radiation-induced lung damage using serial CT imaging and pulmonary function tests, Radiother. Oncol. 148 (2020) 89–96, https://doi.org/10.1016/j.radonc.2020.03.026.
[4] M.A. Olivares-Urbano, C. Griñán-Lisón, J.A. Marchal, M.I. Núñez, "CSC Radioresistance, A therapeutic challenge to improve radiotherapy effectiveness in cancer, Cells 9 (7) (2020) 1–35, https://doi.org/10.3390/cells9071651.
[5] L.B. Marks, X. Yu, Z. Vujaskovic, W. Small, R. Folz, M.S. Anscher, Radiation-induced lung injury, Semin. Radiat. Oncol. 13 (3) (2003) 333–345, https://doi.org/10.1016/S1053-4296(03)00034-1.
[6] L.F. Ye, et al., Radiation-induced lipid peroxidation triggers ferroptosis and synergizes with ferroptosis inducers, ACS Chem. Biol. 15 (2) (2020) 469–484, https://doi.org/10.1021/acschembio.9b00939.
[7] Y. Shibata, H. Yasui, K. Higashikawa, N. Miyamoto, Y. Kuge, Erastin, a ferroptosis-inducing agent, sensitized cancer cells to X-ray irradiation via glutathione starvation in vitro and in vivo, PLoS One 14 (12) (2019) 1–12, https://doi.org/10.1371/journal.pone.0225931.
[8] X. Pan, et al., Erastin decreases radioresistance of NSCLC cells partially by inducing GPX4-mediated ferroptosis, Oncol. Lett. 17 (3) (2019) 3001–3008, https://doi.org/10.3892/ol.2019.9888.
[9] X. Li, X. Zhuang, T. Qiao, Role of ferroptosis in the process of acute radiation-induced lung injury in mice, Biochem. Biophys. Res. Commun. 519 (2) (2019) 240–245, https://doi.org/10.1016/j.bbrc.2019.08.165.
[10] X. Li, L. Duan, S. Yuan, X. Zhuang, T. Qiao, J. He, Ferroptosis inhibitor alleviates Radiation-induced lung fibrosis (RILF) via down-regulation of TGF-β1, J. Inflamm. 16 (1) (2019) 1–10, https://doi.org/10.1186/s12950-019-0216-0.
[11] G. Lei, et al., The role of ferroptosis in ionizing radiation-induced cell death and tumor suppression, Cell Res. 30 (2) (2020) 146–162, https://doi.org/10.1038/s41422-019-0263-3.
[12] S.J. Dixon, et al., Ferroptosis: an iron-dependent form of nonapoptotic cell death, Cell 149 (5) (2012) 1060–1072, https://doi.org/10.1016/j.cell.2012.03.042.
[13] Y. Jiao, Y. Wang, S. Guo, G. Wang, Glutathione peroxidases as oncotargets, Oncotarget 8 (45) (2017) 80093–80102, https://doi.org/10.18632/oncotarget.20278.
[14] A. Bansal, M. Celeste Simon, Glutathione metabolism in cancer progression and treatment resistance, J. Cell Biol. 217 (7) (2018) 2291–2298, https://doi.org/10.1083/jcb.201804161.
[15] L. Yang, et al., Broad spectrum deubiquitinase inhibition induces both apoptosis and ferroptosis in cancer cells, Front. Oncol. 10 (2020) 1–15, https://doi.org/10.3389/fonc.2020.00949. June.
[16] N. Traverso, et al., Role of glutathione in cancer progression and chemoresistance, Oxid. Med. Cell. Longev. 2013 (2013), https://doi.org/10.1155/2013/972913.

[17] S.K. NaveenKumar, M. Hemshekhar, K. Kemparaju, K.S. Girish, Hemin-induced platelet activation and ferroptosis is mediated through ROS-driven proteasomal activity and inflammasome activation: protection by Melatonin, Biochim. Biophys. Acta (BBA) - Mol. Basis Dis. 1865 (9) (2019) 2303–2316, https://doi.org/10.1016/j.bbadis.2019.05.009.

[18] K. Igarashi, M. Watanabe-Matsui, Wearing red for signaling: the heme-bach axis in heme metabolism, oxidative stress response and iron immunology, Tohoku J. Exp. Med. 232 (4) (2014) 229–253, https://doi.org/10.1620/tjem.232.229.

[19] J. Sun, et al., Hemoprotein Bach1 regulates enhancer availability of heme oxygenase-1 gene, EMBO J. 21 (19) (2002) 5216–5224, https://doi.org/10.1093/emboj/cdf516.

[20] H.J. Warnatz, et al., The BTB and CNC homology 1 (BACH1) target genes are involved in the oxidative stress response and in control of the cell cycle, J. Biol. Chem. 286 (26) (2011) 23521–23532, https://doi.org/10.1074/jbc.M111.220178.

[21] K.J. Hintze, Y. Katoh, K. Igarashi, E.C. Theil, Bach1 repression of ferritin and thioredoxin reductase1 is heme-sensitive in cells and in vitro and coordinates expression with heme oxygenase1, β-globin, and NADP(H) quinone (Oxido) reductase1, J. Biol. Chem. 282 (47) (2007) 34365–34371, https://doi.org/10.1074/jbc.M700254200.

[22] A.L. Furfaro, et al., The Nrf2/HO-1 Axis in cancer cell growth and chemoresistance, Oxid. Med. Cell. Longev. (2016) 2016, https://doi.org/10.1155/2016/1958174. Table 1.

[23] L.C. Chang, S.K. Chiang, S.E. Chen, Y.L. Yu, R.H. Chou, W.C. Chang, Heme Oxygenase-1 Mediates BAY 11–7085 Induced Ferroptosis, vol. 416, " *Cancer Lett.*, 2018, pp. 124–137, https://doi.org/10.1016/j.canlet.2017.12.025.

[24] M.Y. Kwon, E. Park, S.J. Lee, S.W. Chung, Heme oxygenase-1 accelerates erastin-induced ferroptotic cell death, Oncotarget 6 (27) (2015) 24393–24403, https://doi.org/10.18632/oncotarget.5162.

[25] S. Imoto, et al., After haemin treatment intracellular non-haem iron increases prior to haem oxygenase-1 induction: a study in human monocytic cell line THP-1, Transfus. Apher. Sci. 58 (6) (2019) 102662, https://doi.org/10.1016/j.transci.2019.10.004.

[26] J. Wan, H. Ren, J. Wang, Iron toxicity, lipid peroxidation and ferroptosis after intracerebral haemorrhage, Stroke Vasc. Neurol. 4 (2) (2019) 93–95, https://doi.org/10.1136/svn-2018-000205.

[27] P. Arosio, S. Levi, Biochimica et Biophysica Acta Cytosolic and mitochondrial ferritins in the regulation of cellular iron homeostasis and oxidative damage, BBA - Gen. Subj. 1800 (8) (2010) 783–792, https://doi.org/10.1016/j.bbagen.2010.02.005.

[28] C.G. Pham, et al., Ferritin heavy chain upregulation by NF-κB inhibits TNFα-induced apoptosis by suppressing reactive oxygen species, Cell 119 (4) (2004) 529–542, https://doi.org/10.1016/j.cell.2004.10.017.

[29] Y. Tian, et al., FTH1 inhibits ferroptosis through ferritinophagy in the 6-OHDA model of Parkinson's disease, Neurotherapeutics (2020), https://doi.org/10.1007/s13311-020-00929-z.

[30] M. Di Sanzo, B. Quaresima, F. Biamonte, C. Palmieri, M.C. Faniello, FTH1 pseudogenes in cancer and cell metabolism, Cells 9 (12) (2020) 1–17, https://doi.org/10.3390/cells9122554.

[31] G. Mesquita, et al., H-Ferritin is essential for macrophages ' capacity to store or detoxify exogenously added iron, 2020, pp. 1–15, https://doi.org/10.1038/s41598-020-59898-0.

[32] G. Zhao, P. Arosio, N.D. Chasteen, Iron(II) and hydrogen peroxide detoxification by human H-chain ferritin. An EPR spin-trapping study, Biochemistry 45 (10) (2006) 3429–3436, https://doi.org/10.1021/bi052443r.

[33] X. Chen, C. Yu, R. Kang, D. Tang, Iron Metabolism in Ferroptosis, vol. 8, October, 2020, pp. 1–14, https://doi.org/10.3389/fcell.2020.590226.

[34] A. Salatino, et al., H-ferritin affects cisplatin-induced cytotoxicity in ovarian cancer cells through the modulation of ROS, Oxid. Med. Cell. Longev. (2019), https://doi.org/10.1155/2019/3461251, 2019.

[35] X. Sun, et al., Activation of the P62-Keap1-NRF2 Pathway Protects against Ferroptosis in Hepatocellular Carcinoma Cells, ", 2015, pp. 173–184, https://doi.org/10.1002/hep.28251.

[36] T. Jansen, A. Daiber, Direct antioxidant properties of bilirubin and biliverdin. Is there a role for biliverdin reductase? Front. Pharmacol. 3 (2012) 1–10, https://doi.org/10.3389/fphar.2012.00030. MAR, no. March.

[37] T.W. Sedlak, M. Saleh, D.S. Higginson, B.D. Paul, K.R. Juluri, S.H. Snyder, Bilirubin and glutathione have complementary antioxidant and cytoprotective roles, Proc. Natl. Acad. Sci. U.S.A. 106 (13) (2009) 5171–5176, https://doi.org/10.1073/pnas.0813132106.

[38] D.E. Barañano, M. Rao, C.D. Ferris, S.H. Snyder, Biliverdin reductase: a major physiologic cytoprotectant, Proc. Natl. Acad. Sci. U.S.A. 99 (25) (2002) 16093–16098, https://doi.org/10.1073/pnas.252626999.

[39] Y.S. Choo, Z. Zhang, in: "Detection of Protein Ubiquitination," No. August, 2009, pp. 10–11, https://doi.org/10.3791/1293.

[40] S.R. Robinson, et al., Hemin toxicity : a preventable source of brain damage following hemorrhagic stroke Hemin toxicity : a preventable source of brain damage following hemorrhagic stroke, 2013, https://doi.org/10.1179/135100009X12525712409931, 0002.

[41] J.P. Friedmann Angeli, et al., Inactivation of the ferroptosis regulator Gpx4 triggers acute renal failure in mice, Nat. Cell Biol. 16 (12) (2014) 1180–1191, https://doi.org/10.1038/ncb3064.

[42] T.M. Seibt, B. Proneth, M. Conrad, Role of GPX4 in ferroptosis and its pharmacological implication, Free Radic. Biol. Med. 133 (2019) 144–152, https://doi.org/10.1016/j.freeradbiomed.2018.09.014.

[43] W. S. Yang et al., "Regulation of ferroptotic cancer cell death by GPX4," Cell, vol. 156, no. 1–2, pp. 317–331, Jan. 2014, doi: 10.1016/j.cell.2013.12.010.

[44] I. Ingold, et al., Selenium utilization by GPX4 is required to prevent hydroperoxide-induced ferroptosis, Cell 172 (3) (2018) 409–422, https://doi.org/10.1016/j.cell.2017.11.048, e21.

[45] C. Wiel et al., "BACH1 stabilization by antioxidants stimulates lung article BACH1 stabilization by antioxidants stimulates lung cancer metastasis," Cell, vol. 178, no. 2, pp. 330-345.e22, doi: 10.1016/j.cell.2019.06.005.

[46] X. Sui, R. Zhang, S. Liu, T. Duan, L. Zhai, RSL3 drives ferroptosis through GPX4 inactivation and ROS production in colorectal cancer 9 (2018) 1–8, https://doi.org/10.3389/fphar.2018.01371. November.

[47] S.H. Lecker, A.L. Goldberg, W.E. Mitch, in: Protein Degradation by the Ubiquitin – Proteasome Pathway in Normal and Disease States vol. 11, 2006, pp. 1807–1819, https://doi.org/10.1681/ASN.2006010083.

[48] B. Perillo, M. Di Donato, A. Pezone, E. Di Zazzo, G. Castoria, A. Migliaccio, ROS in cancer therapy : the bright side of the moon, Exp. Mol. Med. (2020) 192–203, https://doi.org/10.1038/s12276-020-0384-2.

[49] T.W.R. Hansen, R.J. Wong, D.K. Stevenson, X.T.W.R. Hansen, R.J. Wong, D. K. Stevenson, Physiological Reviews MOLECULAR PHYSIOLOGY and PATHOPHYSIOLOGY of BILIRUBIN HANDLING by the BLOOD , LIVER , INTESTINE , and BRAIN IN the NEWBORN PATHOPHYSIOLOGY of BILIRUBIN HANDLING by the BLOOD , LIVER , INTESTINE , and BRAIN IN the NEWBORN, 2021, pp. 1291–1346, https://doi.org/10.1152/physrev.00004.2019.

[50] E. Park, S.W. Chung, ROS-mediated autophagy increases intracellular iron levels and ferroptosis by ferritin and transferrin receptor regulation, Cell Death Dis. (2019), https://doi.org/10.1038/s41419-019-2064-5.

[51] H. Nishizawa, et al., Cro Ferroptosis is controlled by the coordinated transcriptional regulation of glutathione and labile iron metabolism by the transcription factor BACH1 295 (2020) 69–82, https://doi.org/10.1074/jbc.RA119.009548.